《Original》

Calculation of Power Distributions on Uranium- and Plutonium-Loaded Cores Moderated by Light Water

Sang Keun Lee, Kap Suk Moon, Jong-Hwa Jang

Ji Bok Lee and Chang Kun Lee

Korea Advanced Energy Research Institue

우라늄 및 플루토늄 장전 노심에서의 출력 분포 계산

이상근 · 문갑석 · 장종화 · 이지복 · 이창건

한국에너지연구소

Abstract

An analytical system has been established for scrutinizing both uranium- and plutonium-fueled lattices moderated by light water. This system consists of two primary codes. One is a unit cell program called KICC, which has theoretical foundation on the models of GAM and THERMOS incorporated with appropriate approximate treatments for various phenomena, whereas the other is a multi-dimensional diffusion-depletion program entitled KIDD.

The adequacy of this system is verified by performing extensive benchmark calculations on a variety of critical exeperiments. The average value of effective multiplication factors for the selected nineteen UO_2 critical experiments of heterogeneous lattice structure is calculated to be 1.0006 with a standard deviation of 0.0039. Power distributions have also been calculated for some critical experiments fueled with both uranium and plutonium of varying concentrations. The maximum percentage difference between the measured and calculated power distributions appears to be less than 5%. This result, together with the previously reported result, illustrates that the KICC/KIDD system is a very effective tool for the analysis of a light water reactor core.

요 약

우라늄 및 플루토늄을 핵연료로 이용하고 경수를 감속재로 쓰는 원자로에 대한 해석적 체제를 수립하였다. 이 체제는 두개의 주요 전산코드로 구성되어 있는 바, 하나는 단위격자 세포코드인 KICC로서 이는 GAM 및 THERMOS의 이론적인 기초에 여러가지 현상을 적절하게 표현할 수 있는 근사식을 결합한 것이다. 다른 하나는 다차원 확산—연소 방정식코드인 KIDD이다.

이 체제는 다양한 종류의 임계실험로에 대하여 철저한 검증계산을 수행하므로써 그 신뢰성을 입증하였다. 즉 서로 다른 노심구조를 가진 19가지의 비균질 임계실험로에 대하여 유효증배계수를 계산한 결과 이의 평균치 1.0006, 표준편차 0.0039로서 잘 일치하였다. 또한 우라늄과 플루토늄을 핵

연료로 사용하는 여러종류의 임계로에 대하여 출력분포를 계산하여 측정치와 비교하였으며 계산치는
최대 오차 ±5%이내에서 측정치에 일치하였다. 이러한 사실은 KICC/KIDD체제가 경수로의 해석에
아주 유용한 도구가 됨을 밝혀 준다.

I. Introduction

Recycling of plutonium in thermal power reactor has significant conservation advantaages. It reduces the requirements for uranium ore, and for separative work at uranium enrichment plants.

Valid technical bases for design and management of plutonium reloads which are based upon a thorough knowledge of the neutronic behavior of plutonium-fueled system should be established as a fact *a priori*. The adequacy of analytic models and computer programs used to predict the behavior of nuclear reactors is deter mined by analyzing simplified configuration experiments referred to as benchmarks. Reactor core and lattice physics programs, in particular, must be benchmarked against a wide range of critical lattice experiments representative of various operating conditions.

At present, the number of clean-critical lattice experiments using uranium oxide fuel can be found in numerous literatures, and the design methods that have been normalized for uranium cores seem to be adequate. The number of such experiments fueled by mixed oxide (UO_2-PuO_2) fuel, however, is much more limited and subject to greater experimental uncertainties.

An analytical method using KICC/KIDD code system has been established for the prediction of neuronic behavior in light water reactor loaded with both uranium oxide and mixed oxide fuels. For the cell callculation of plutoni um-bearing fuel moderated by light water a program, KICC[1], has been developed.

The objective of this work is to confirm the validity of the code system by extensive bench-mark calculations upon a wide variety of critical lattice experiments. The adequacy of this system for the calculation of effective multiplication factors for uniform lattices of mixed oxide fuel system had been presented in the previous reoprt.[2] In this report we present results of the effective multiplication factor for lattices whose spatical uniformity is interrupted by discontinuities such as water thimbles and control elements. Also presented herein are thearesults of power distributions of plutonium-fueled light water moderated critical experiments. These experiments include great variety in uranium-plutonium contents, plutonium isotope concentrations, lattice pitch, and extent of moderator posoning. Power distributions have been calcuated for both single-region and multi-region cores. The core configurations can be arranged in four categories: namely, single region uniform cores, single region perturbed cores, concentric multi-region cores, and salt and pepper cores. Single region perturbed cores have such core configurations as

1) A central test position formed by removing a fuel rod in the center of the core,

2) A five-rod slot pattern formed by removing five rods in a row in the center of the core,. and

3) 41 Vicor rods are distributed at regular interval replacimg the fuel rods in these positions.

Prediction of power distributinos to within about 5% and core reactivity to within 0.5% has been the prime target throughout the process of our benchmark calculations.

II. Computational Methods

Two kinds of calculations have been per-

formed: unit cell calculations and reactor (full core) calculations. The primary codes utilized for these purposes were KICC and KIDD[3], respectively. KICC, formerly KARATE, has been utilized to perform a spectrum calculation and to create broad group cross sections, while KIDD has been utilized for the calculation of rodwise power distributions and reactor reactivity.

1. Cell Calculations

Unit cell calculations have been performed using the geometrical dimensions of the cell and nuclear densities of the various nuclides. KICC, which has been developed to compute the neutron spectra in space and energy in a cylindrical unit cell is used for these purposes. It is based upon the theoretical models of GAM[4], THERMOS[5], and CINDER[6] and incorporatas the various approximate treatments known to be accurate. Some of the approximate treatments incorporated into KICC program are as follows:

One of the prime objectives of the cell calculation is to generate a correct neutron spectrum, which in turn can be be used to generate accurate broad group cross sections for reacto rcalculations. A very important feature of this calculation is the accuracy with which the resonance calculation is performed. The WIMS treatment[7] has been adopted which employs tables of groupwise resonance integrals as a function of temperature and potential scattering and relies on the resonance equivalence theorems to interpolate within the table in the determination of the resonance integral appropriate for a given situation.

In the mixed oxide fuels, the overlap of resonances of uranium isotopes and plutonium isotopes causes a reduction in the resonance integrals and thus, causes an increase in the effective multiplication factor. This effect has been approximated utilizing the WIMS[8] method when the fuel is made up of mixed oxide.

The ability to predict the effect of plutonium oxide particle size has on the neutron multiplication of a reactor system is important for economic utilization of plutonium. The reactivity effect of changing the plutonium oxide particle size in a water-moderated UO_2-PuO_2 fueled lattice is complex because of the interaction of changes in Pu-239 fission, Pu-239 capture and Pu-240 absorption reaction rates. Self-shielding of Pu-239 with increasing PuO_2 particle size reduces the Pu-239 fission reaction rate in the fuel, but also reduces the Pu-239 capture-to-fission ratio due to a larger proportionate increase in shielding of the 0.3 eV resonance.. Increased shielding of the 1.0 eV resonance of Pu-240 with increasing PuO_2 particle size contributes a positive reactivity effect. The magnitude of this positive reactivity effect is dependent on the isotopic fraction of Pu-240 in plutonium. Combinations of the positive and negative reactivity effects due to PuO_2 particle shielding can result in either increase or decrease in the net reactivity, depending on the neutron spectrum, the relative Pu-240 content of the plutonium, and the change in the PuO_2 particle size. An approximate method to treat this effect devised by Windsor and Goldstein[9] has been utilized where applicable.

KICC computes the thermal neutron spectrum in space and energy in a cylindrical unit cell composed of up to ten material regions. Space point designation and material placement in each region is quite flexible. The fuel cell was considered to be made up of three material regions: fuel, cladding, and moderator.Nineteen space points describe this unit cell with eight being allocated to the fuel,one to the cladding, and ten to the moderator. White boundary conditions[10] at the outer boundary were simulated by assuming the cell to be surrounded by a

fictitious scattering ring.Two space points were also allocated to the scattering ring.The poison cell in which fuel is replaced by absorber material such as Vicor or aluminum, was treated similarly, i.e., absorber, cladding and moderator. Thirteen space points describe this unit cell with eight being allocated to the absorber, one to the cladding and four to the moderator. White boundary conditions were also assumed at the outer boundary. Unit cell calculations have been also performed for water thimble and reflector.

A four broad group representation has been used throughout the analysis. This four group structure is bound by the energy points: 10 MeV, 0.821 MeV, 5530 eV, 0.625 eV and 0.0 eV. The mixed number density model has been used to obtain thermal neutron cross sections below energy of 0.625 eV. This is consistent with the previous analysis.

2. Reactor Calculations

The spatial and energy-dependent calculations

for the full reactors have been performed using the KIDD program. This program solves the few-group neutron diffusion equation in one, two and three space dimensions for its lowest eigenvalue and corresponding direct and/or adjoint vectors, in both multiplying and non-multiplying system.

Because the core configurations are not homogenenous in reactivity problem, and the power measurements were made for some fuel rods in the fixed positions, the reactor calculations have been performed in X-Y two dimensions. A mesh point has been allocated per pin cell, and sufficient number of mesh points has been given to the reflector region.

III. Results and Discussions

1. Effective Multiplication Factors for Heterogeneous Reactors

In order to verify the adequacy of KICC/KIDD systems in predicting the effective multiplication factors of heterogeneous systems, nine-

Table 1. Critical Conditions of Major Assemblies

Core No.	Run No.	Number of Fuel Rods	Enrichment (w/o)	Number of Poison Rods	Poison Density (%)	Type of Poison	Moderator Height (cm)	Boron Concentration (ppm)
0	5	332	4.02	0	0	—	174.9	0
0	10	376	4.02	0	0	—	90.7	0
0	12	500	4.02	0	0	—	55.6	0
7	73	472	4.02	45	9	Vicor	95.7	0
7	78,80	424	4.02	41	9	Vicor	141.0	0
7	88	424	4.02	40	9	Vicor	127.3	0
7	215	424	4.02	41	9	Moderator	145.0	392.0
8	74	500	4.02	69	12	Vicor	111.3	0
8	75	472	4.02	65	12	Vicor	142.6	0
8	209	472	4.02	65	12	Aluminum	155.2	474.3
8	211	472	4.02	65	12	Moderator	106.6	474.3
8	212	472	4.02	65	12	Moderator	159.7	558.0
9	103	690	2.46	67	9	Vicor	134.4	0
9	104	690	2.46	66	9	Vicor	122.2	0
9	106	868	2.46	121	12	Vicor	139.2	0
9A	23	428	2.46	0	0	—	171.7	0
9A	24	416	2.46	25	6	Moderator	139.3	0
9A	25	424	2.46	57	12	Moderator	83.8	0
9A	26	368	2.46	49	12	Moderator	170.2	0

teen critical experiments conducted at Babcock and Wilcox[11] have been chosen as benchmarks. These experiments represent the cores that have a fairly broad range of poison rod densities, including those of interest for practical light water moderated power reactors. The nominal poison rod densities are 0, 6, 9, and 12%, where poison rod density is defined as the percentage of poison rods to total rods in the core. Table 1 summarizes the critical conditions of each experiment. Cores contain either stainless steel clad 4.06% enriched UO_2 fuels or aluminum clad 2.46% enriched UO_2 fuels. The physical properties of the fuel rods are given in Table 2. The lumped poison rods are Pyrex rods depleted in boron (Vicor) and solid aluminum rods. The physical properties of the poison rods are presented in Table 3. These poison rods are distributed throughout the core

at regular intervals.

The adequacy of our calculational system in predicting the effective multiplication factors for these critical experiments is shown in Table 4. The average value of the offective multiplication factors for these nineteen heterogeneous systems is calculated as 1.0006 with a standard deviation of 0.0039.

The reactivity worth of central Vicor poison rod has also been calculated and compared with the measured value. In experiment the reactivity worths of Vicor rods were measured by removing a central Vicor poison rod from the Core-7 Run-78 and Core-9 Run-103, respectively, and then reaching criticality again by lowering the height of moderator. In our calculation, effective multiplication factors have been calculated by replacing a central Vicor poison rod with moderator. Measurements

Table 2. Physical Properties of BAW UO_2 Fuel Rods

Property	4.02% UO_2	2.46 % UO_2
Outer diameter, in	0.4755 ± 0.0015	0.4748 ± 0.0006
Wall thickness, in	0.0160 ± 0.0005	0.032 ± 0.001
Wall material	304 Stainless Steel	6061 Aluminum
Pellet Diameter, in	0.444 ± 0.002	0.4054 ± 0.005
Active Fuel length, in	66.7 ± 0.3	60.37 ± 0.35
Weight of fuel, gm/rod	$1,600\pm2$	$1,306\pm1$
Weight % of U in UO_2	88.01 ± 0.02	88.13 ± 0.001
Weight of U-235, gm/rod	56.61 ± 0.10	28.42 ± 0.02
U-235 Enrichment, w/o	4.020 ± 0.005	2.459 ± 0.002
Fuel density, gm/cm^3	9.46 ± 0.10	10.24 ± 0.04

Table 3. Properties of Poison Rods

Property	Vicor	Aluminum
Outer diameter, cm	1.115 ± 0.001	1.111 ± 0.001
Wall thickness, cm	0.0904 ± 0.0004	—
Wall material	6061 Aluminum	—
Poison diameter, cm	0.825 ± 0.001	1.111 ± 0.001
Total length,	183.6 ± 0.1	183.0 ± 0.5
Weight of poison, gm	214.5 ± 0.5	478.0 ± 0.5
Poison analysis:		
B_2O_3, wt %	3.035	—
Boron, wt %	0.943	—

Table 4. Calculated Values of Effective Multiplication Factor for Babcock and Wilcox Critical Assemblies

Core No.	Run No.	Buckling (m^{-2})	K_{eff}
0	5	2.950	0.9950
0	10	9.468	0.9997
0	12	2.192	1.0013
7	73	8.604	1.0031
7	78, 80	4.317	0.9991
7	215	4.113	1.0036
8	74	6.566	1.0042
8	75	4.236	1.0024
8	209	3.647	1.0035
8	211	7.112	1.0078
8	212	3.468	1.0054
9	103	4.701	0.9958
9	106	4.416	0.9953
9 A	23	3.056	0.9947
9 A	24	4.416	0.9972
9 A	25	1.098	1.0018
9 A	26	3.101	1.0007

Mean $K_{eff}=1.0006\pm0.0039$

showed that the worths of a central Vicor poison rod were 41 cent and 42 cent, while our calculational results for each case were 46 cent and 47.6 cent, respectively.

2. Power Distributions

Power distributions have been calculated for all twelve EPRI critical cores[12] and seventeen ESADA Plutonium Program critical cores[13] that the relative power distributions were measured. A power distribution measured by Babcock and Wilcox[14] is also included in the analysis. In this paper, however, results of only nine cases considered to be representative of various core configurations are presented.

2.1. EPRI Critical Cores

The purpose of the experimental measurements reported in EPRI-NP-196 is to provide benchmark neutronic data in assessing the accuracy of neutronic analysis methods for both slightly enriched uranium lattices and mixed oxide lattices. The relative power distribution

Table 5. 2.35 % Enriched UO₂ Fuel Specifications

FUEL RODS
1. Rod Dimensions
   Outer diameter:　　　0.500 inch
   Wall thickness:　　　0.030 inch
   Fuel diameter:　　　0.440 inch
   Overall fuel length:　38.5 inches
   Active fuel length:　36.0 inches
2. Cladding: 6061 aluminum tubing seal welded with a lower end plug of 5052-H32 aluminum and a top plug of 1100 aluminum
3. Total weight of loaded fuel rods: 917 gm (average)

FUEL LOADING
1. Fuel mixture vibrationally compacted
2. 825 gm of UO₂ powder/rod, 726 gm of U/rod, 17.08 gm of U-235/rod
3. Enrichment: 2.35±0.05 w/o U-235
4. Fuel density: 9.20 gm/cm³ (84 % theoretical density).

Table 6. UO₂-2 wt % PuO₂ Fuel Specifications

FUEL RODS
1. Rod Dimensions
   Outer diameter:　　　0.565 inch
   Wall thickness:　　　0.030 inch
   Fuel diameter:　　　0.505 inch
   Overall fuel length:　36.60 inches
   Active fuel length:　36.00 inches
2. Cladding: Zircaloy-2 tubing with plugs seal welded at both ends
3. Total weight of loaded fuel rods: 1340 gms (average)

FUEL LOADING
1. PuO₂ mixed in natural UO₂ and vibrationally compacted
2. 1128 gms of UO₂-PuO₂ mixture/rod
3. Chemical composition wt %: Pu/PuO₂=88.1, U/UO₂=88.0, Pu/mixture=1.760
4. PuO₂ is 2.00 wt % of total mixture
5. Fuel density: 9.54 gm/cc (about 87 % theoretical density)
6. UO₂ power at the end of fuel column
7. The isotopic distribution of plutonium: 91.615 Pu-239, 7.654 Pu-240, 0.701 Pu-241, 0.031 Pu-242
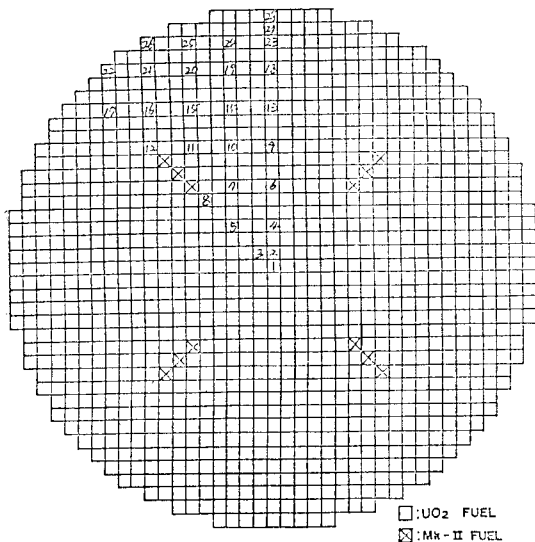8. Analysis date: January 1965.

Fig 1. Core Diagram for a Cylindrical Single-Region Core Poisoned with 463.8 ppm Boron, 2.35% Enriched UO_2 Fuel, 0.615-inch Lattice (Core E2)
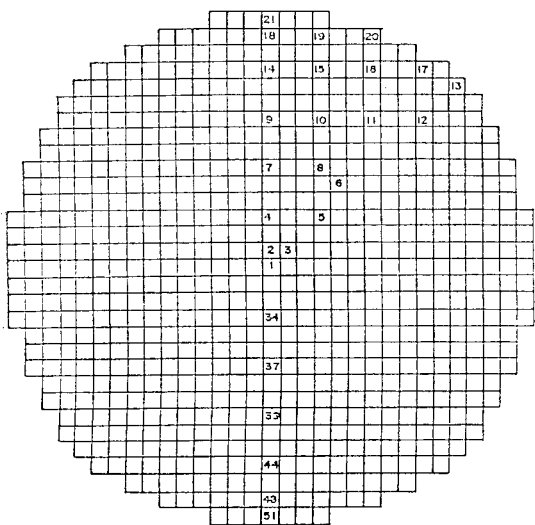

Fig 2. Core Diagram for a Cylndrical Single-Region Core Poisoned with 687.9 ppm Boron, 8% Pu-240 Fuel, 0.70-inch Lattice (Core E8)

in a given array was determined from an analysis of measurements of the fission product gamma ray intensity from the fuel, rod-to-rod, throughout each array. Each fuel rod selected for measurements was counted on a dual channel counting system, which automatically

corrected for fission product decay during the measurement period.

The twelve experiments consist of six lattices containing 2.35% enriched UO_2 fuel and six lattices containing natural UO_2-2 wt% PuO_2 (8% Pu-240). The specifications of UO_2 fuel and mixed oxide fuel are presented in Table 5 and in Table 6, respectively. Two of the core configurations presented in this paper are shown in Figures 1 and 2. One is for a typical single region UO_2 core and the other is for mixed oxide. Both cores are poisoned with natural boron. Numbers in the figures indicate the positions where measurements were made.

The calculated power distributions are compared with the measured ones for each core

Table 7. Relative Power Production of Core E2

Rod Number	Measured	Calculated	% Difference
1	1.5294±0.0162	1.5333	−0.3
2	1.5051±0.0159	1.5333	−1.9
3	1.5109±0.0160	1.5333	−1.5
4	1.4832±0.0111	1.4952	−0.8
5	1.4502±0.0154	1.4667	−1.1
6	1.3987±0.0149	1.4000	−0.1
7	1.3714±0.0146	1.3619	0.7
8	1.3503±0.0144	1.3238	2.0
9	1.2438±0.0094	1.2381	0.5
10	1.2194±0.0130	1.2100	0.8
11	1.0878±0.0120	1.1048	−1.6
12	0.9542±0.0100	0.9524	0.2
13	1.0230±0.0120	1.0286	−0.5
14	1.0000	1.0000	0.0
15	0.9198±0.0101	0.9143	0.6
16	0.7883±0.0087	0.7819	0.8
17	0.6467±0.0073	0.6333	2.0
18	0.8012±0.0063	0.7838	2.2
19	0.7547±0.0084	0.7581	−0.5
20	0.7039±0.0075	0.6886	2.2
21	0.6260±0.0071	0.6124	2.2
22	0.7491±0.0083	0.8133	−8.6
24	0.6450±0.0073	0.6143	4.8
25	0.6351±0.0072	0.6200	3.3
26	0.8031±0.0089	0.8600	−7.1
27	0.6099±0.0069	0.6095	0.0
28	0.7105±0.0056	0.7638	−7.5

Table 8. Relative Power Production of Core E8

Rod Number	Measured	Calculated	% Difference
1	1.4747±0.0111	1.4623	0.8
2	1.4625±0.0110	1.4528	0.7
3	1.4584±0.0110	1.4528	0.4
4	1.4366±0.0077	1.4057	2.2
5	1.3534±0.0102	1.3585	−0.4
6	1.2329±0.0094	1.2453	−1.0
7	1.2794±0.0069	1.2642	1.2
8	1.1999±0.0119	1.2170	−1.4
9	1.0384±0.0057	1.0377	0.1
10	1.0000	1.0000	0.0
11	0.8717±0.0068	0.8774	−0.7
12	0.6894±0.0056	0.6915	−0.3
13	0.7414±0.0062	0.8613	−16.2
14	0.7444±0.0042	0.7575	−1.8
15	0.7203±0.0058	0.7236	−0.5
16	0.6456±0.0053	0.6387	1.1
17	0.6922±0.0056	0.7575	−9.4
18	0.6047±0.0035	0.6085	−0.6
19	0.6299±0.0052	0.6623	−5.1
20	0.8504±0.0067	1.0189	−19.8
21	0.7251±0.0041	0.8311	−14.6

configuration in Table 7 and 8. The calculated power is normalized to a rod power where the measured power was normalized. As can be seen in the tables, calculated powers agree with the measured values within ±4% except for core periphery which forms core-reflector boundary. Power distributions are also calculated and compared with measured values for the other ten core configurations that are not presented in this paper. In summary, the maximum difference between the measured and the calculated powers is less than 4%.

2.2. ESADA Critical Cores

In ESADA experiments, power distribution measurements were made by relating the fission product gamma activity of irradiated fuel rods to the temperature rise of the fuel clad surface which is proportional to the rod power. Low background fuel rods were placed in the core, irrradiated, and the resulting fission product activity counted with a well collimated gamma
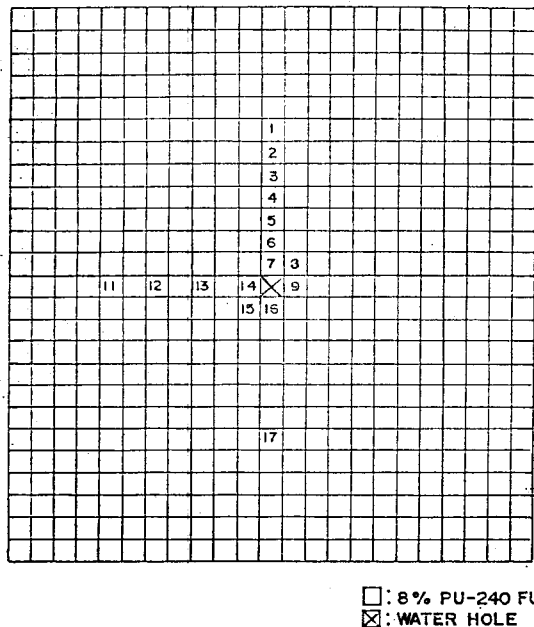

□ : 8 % PU-240 FU
☒ : WATER HOLE

Fig 3. Core Diagram for a 23×25 Single-Region Core with Center Water Hole—8% Pu-240 Fuel, 0.69-inch Lattice (Core C1)

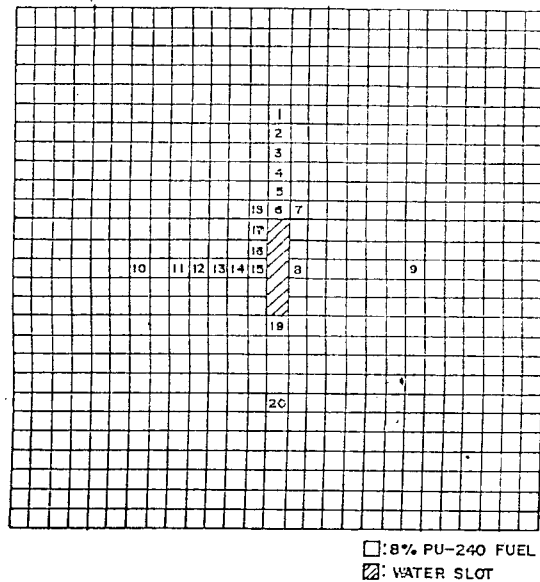□ : 8% PU-240 FUEL
☒ : WATER SLOT

Fig 4. Core Diagram for a Borated 27×27 Single-Region Core with6 Five-Rod Water Slot—8% Pu-240 Fuel, 0.69-inch Lattice, Boron Concentration=315 ppm (Core C4)
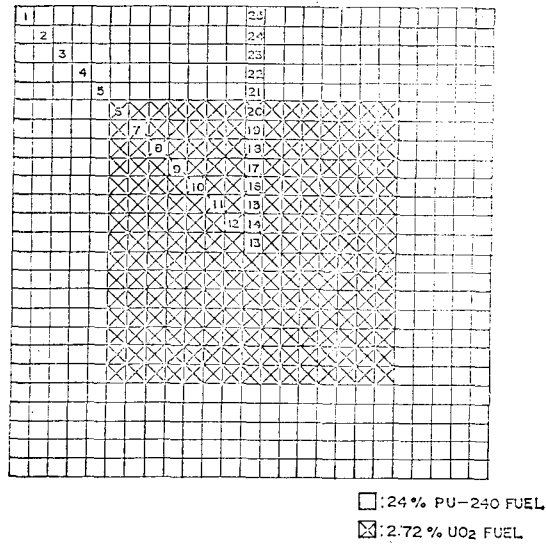
☐:24 % PU–240 FUEL
☒:2.72 % UO₂ FUEL

Fig. 5. Core Diagram for a 25×25 Concentric Multi-Region Core Containing a 15×15 UO₂ Inner Region and a 24% Pu-240 Outer Region, 0.69-inch Lattice (Core C16)

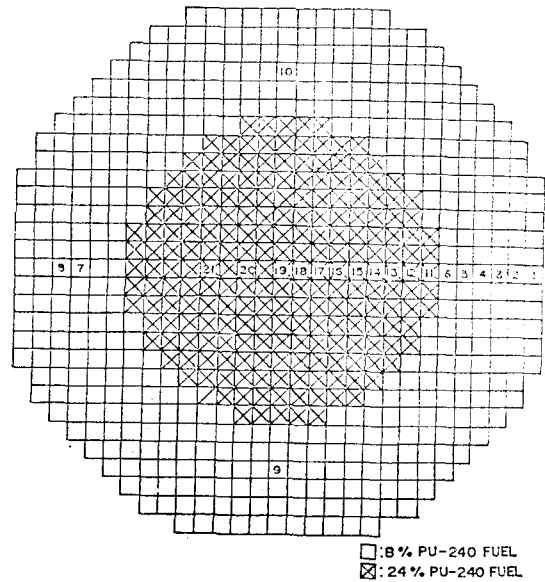☐:8 % PU-240 FUEL
☒:24 % PU-240 FUEL

Fig. 6. Core Diagram for a Concentric Multi-Region Core Containing a 24% Pu-240 Inner Region and an 8% Pu-240 Outer Region, 0.69-inch Latticeo (Cre C18)
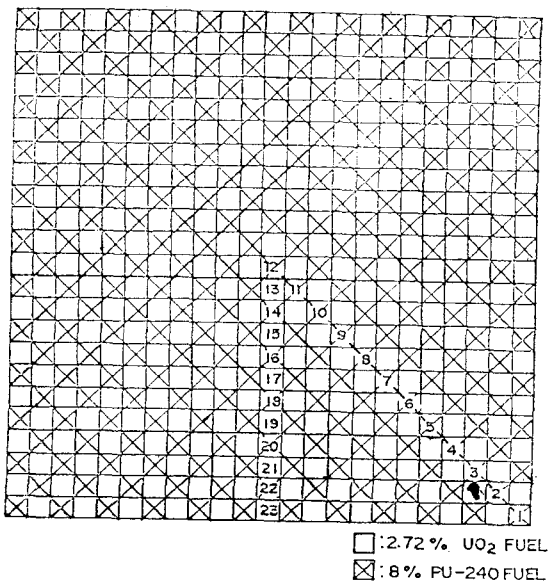

☐:2.72 % UO₂ FUEL
☒:8 % PU-240 FUEL

Fig. 7. Core Ciagram for a 23×23 Salt and Pepper Core Composed of 8% Pu-240 and UO₂ Fuels, 0.69-inch Lattice (Core C22)

☐:24 % PU-240 FUEL
☒:8 % PU-240 FUEL
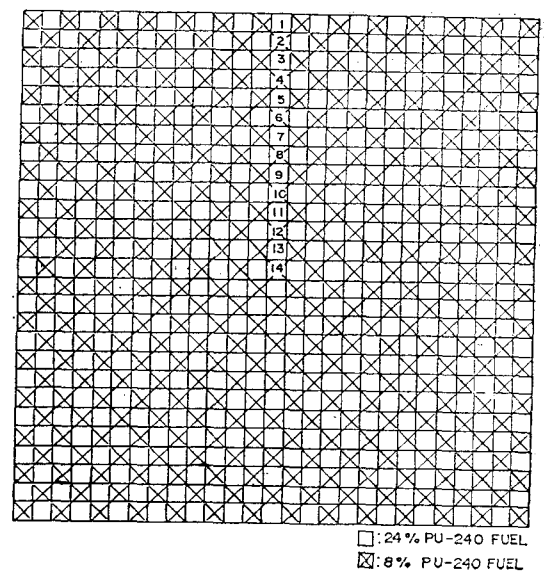
Fig. 8. Core Diagram for a 27×27 Salt and Pepper Composed of 8% Pu-24 and 24% Pu-240 Fuels, 0.69-inch Lattice (Core C21)

scintillation counter.

However, in configurations composed of both uranium and plutonium fuels, it is not possible to determine the correct relative power in each fuel by a gamma scan since the gamma source

and decay characteristics of the two fuels are different. The plutonium and uranium fuel rods used in ESADA experiments had different diameters and the two plutonium fuels had different Pu-240 contents. Consequently, addition-

al heat rate experiments were carried out to permit a re-evaluation of the power-to-gamma activity time-dependent factors. It is, therefore, recommended that the relative power values listed for mixed oxide fuel rods should be multiplied by 1.41 to correct the difference.

Core configurations where comparisons of power distributions were made in this paper are presented in Figures 3 through 8. The first two configurations represent the single region cores perturbed with a water hole or water slot. Water hole was formed by removing a fuel rod in the center of the core, while water slot was formed by removing five rods in a row in the

Table 9. ESADA 2.72 % UO₂ Fuel Specification

• Enrichment, w/o U-235	: 2.72
• Pellet diameter	: 0.400 inch
• Clad outer diameter	: 0.4683 inch
• Active fuel length	: 48.0 inches
• Clad material	: Zircaloy-4
• Density of fuel	: 95% of theoretical
• UO₂/rod	: 1028.02 gms
• U/rod	: 905.93 gms

Table 10. ESADA MOX Fuel Specifications

FUEL RODS

- Fuel outer diameter : 0.505 inch
- Clad outer diameter : 0.565 inch
- Wall thickness   : 0.030 inch
- Active fuel height : 36 inches
- PuO₂ is mixed in natural UO₂
- PuO₂ is 2 wt % of total mixture
- Fuel density   : 9.54 gm/cc

Isotopic Composition of Plutonium :

Isotope	8% Pu-240	24% Pu-240
Pu-239	91.62	71.76
Pu-240	7.65	23.50
Pu-241	0.70	4.08
Pu-242	0.03	0.66

- The PuO₂ particles are not spherical. They were passed through a 325-mesh screens. Their mean diameter is about 25 microns.

Table 11. Relative Power Production of Core C1

Rod Number	Measured	Calculated	% Difference
1	0.808	0.801	0.9
2	0.848	0.853	−0.6
3	0.899	0.898	0.0
4	0.950	0.935	1.6
5	0.973	0.973	0.0
6	1.025	1.025	0.0
7	1.240	1.249	−0.7
8	1.109	1.145	−3.2
9	1.255	1.249	0.5
10	0.775	0.778	−0.4
11	0.790	0.778	1.5
12	0.897	0.883	1.6
13	0.994	0.965	2.9
14	1.266	1.249	1.3
15	1.125	1.145	−1.8
16	1.255	1.249	0.5
17	0.806	0.801	0.6

Table 12. Relative Power Production of Core C4

Rod Number	Measured	Calculated	% Difference
1	0.732	0.737	−0.7
2	0.793	0.790	0.4
3	0.835	0.843	−1.0
4	0.895	0.889	0.7
5	0.968	0.962	0.6
6	1.241	1.241	0.0
7	1.069	1.121	−4.9
8	1.602	1.725	−7.8
9	0.798	0.790	1.0
10	0.809	0.790	2.3
11	0.891	0.883	0.9
12	0.941	0.916	2.7
13	0.988	0.962	2.6
14	1.137	1.088	4.3
15	1.586	1.725	−8.8
16	1.584	1.679	−6.0
17	1.409	1.447	−2.7
18	1.119	1.121	−0.2
19	1.258	1.241	1.4
20	0.812	0.790	2.7

center of the core. Next two core configurations represtnt the concentric multi-region cores. Two types of fuel rods were loaded into the core; one inner zone, the other outer zone. The last

Table 13. Relative Power Production of Core C16

Rod Number	Measured	Calculated	% Difference
1	0.5195	0.6724	−29.4
2	0.3230	0.3375	−4.5
3	0.3354	0.3316	1.1
4	0.4055	0.4027	0.7
5	0.5610	0.5453	2.8
6	0.5681	0.5545	2.4
7	0.9026	0.9158	−1.5
8	1.1009	1.1007	0.0
9	1.2906	1.2789	0.9
10	1.3695	1.3944	−1.8
11	1.5004	1.4769	1.5
12	1.5193	1.5263	−0.5
13	1.5812	1.5428	2.4
14	1.5350	1.5347	0.0
15	1.5113	1.5099	0.1
16	1.4286	1.4687	−2.8
17	1.4244	1.4026	1.5
18	1.3166	1.3201	−0.3
19	1.1967	1.1800	1.4
20	0.9304	0.8910	4.2
21	0.9974	0.9983	−0.1
22	0.7154	0.6816	4.7
23	0.5847	0.5759	1.5
24	0.5666	0.5726	−1.1
25	0.8157	0.9405	−15.3

Table 14. Relative Power Production of Core C18

Rod Number	Measured	Calculated	% Difference
1	1.1531	1.3195	−14.4
2	0.7867	0.7755	1.4
3	0.7827	0.7621	2.6
4	0.8447	0.8307	1.7
5	0.9381	0.9088	3.1
6	1.0030	0.9977	0.5
7	0.8421	0.8307	1.4
8	0.7786	0.7621	2.1
9	0.8665	0.8307	4.1
10	0.8476	0.8307	2.0
11	0.9517	0.9681	−1.7
12	1.0017	1.0368	−3.5
13	1.0652	1.0758	−1.0
14	1.0963	1.1148	−1.7
15	1.1166	1.1445	−2.5
16	1.1247	1.1633	−3.4
17	1.1598	1.1835	−2.0
18	1.1761	1.1929	−1.4
19	1.1977	1.1929	0.4
20	1.1571	1.1835	−2.3
21	1.1098	1.1445	−3.1

Table 15. Relative Power Production of Core C22

Rod Number	Measured	Calculated	% Difference
1	0.7619	1.0322	−35.5
2	0.5846	0.6204	−6.8
3	0.6317	0.6380	−1.0
4	0.7496	0.7575	−1.1
5	0.8911	0.9022	−1.2
6	1.0187	1.0403	−2.1
7	1.1660	1.1703	−0.4
8	1.3116	1.2842	2.1
9	1.4165	1.3736	3.0
10	1.4708	1.4386	2.2
11	1.4924	1.4793	0.9
12	1.5226	1.4955	1.8
13	0.7455	0.7372	1.1
14	1.5011	1.4711	2.0
15	0.7304	0.7095	2.9
16	1.4120	1.3818	2.1
17	0.6561	0.6543	0.3
18	1.2381	1.2516	−1.1
19	0.5739	0.5746	−0.1
20	1.0730	1.0647	0.8
21	0.4788	0.4835	−1.0
22	0.9430	0.9833	−4.2
23	0.6302	0.6811	−8.1

two configurations represent the salt-and-pepper cores where two types of fuel rods were placed in so-called cheker-board type. Physical properties of UO_2 and mixed oxide fuels are given in Table 9 and Table 10, respectively.

Comparisons of the power distributions for each core configuration are given in Tables 11 through 16. Th calculated powers are normalized in such a manner that the least square differences become minimum. As are seen in the tables, the calculated powers agree with the measured values within ±5% in all cases except for the immediate vicinities of water slot and reflector.

2.3. Babcock and Wilcox Critical Core

An additional comparison of power distribution has been carried out for the Babcock and Wilcox critical core. The core was loaded with

Table 16. Relative Power Production of Core C21

Rod Number	Measured	Calculated	% Difference
1	0.9638	1.1752	−21.9
2	0.8018	0.7819	2.5
3	0.6727	0.6831	−1.5
4	0.8557	0.8293	3.1
5	0.7800	0.8104	−3.9
6	0.9941	0.9790	1.5
7	0.8895	0.9280	−4.3
8	1.1473	1.0983	4.3
9	0.9941	1.0218	−3.2
10	1.2132	1.1837	2.4
11	1.0551	1.0898	−3.3
12	1.2826	1.2347	4.4
13	1.0685	1.1153	−4.4
14	1.2861	1.2517	2.7

Fig. 9. Core Diagram of Babcock & Wilcox Critical Core (Core-7 Run-78 & 80)

Table 17. Relative Power Production of Core-7 Run-78 & 80

Rod Number	Measured	Calculated	% Difference
1	1.081	1.080	0.1
2	1.027	1.004	2.2
3	0.969	0.985	−1.7
4	0.946	0.973	−2.9
5	0.893	0.900	−0.8
6	0.837	0.842	−0.6
7	0.777	0.801	−3.1
8	0.710	0.709	0.1
9	0.597	0.622	−4.2
10	0.562	0.578	−2.8
11	0.784	0.818	−4.3
12	1.050	1.076	−2.5
13	1.000	1.000	0.0
14	0.998	0.986	1.2
15	0.972	0.974	−0.2
16	0.881	0.898	−1.9
17	0.827	0.839	−1.5
18	0.773	0.798	−3.2
19	0.691	0.707	−2.3
20	0.612	0.620	−1.3
21	0.548	0.575	−4.6
22	0.784	0.825	−5.2
23	1.026	1.031	−0.5
24	1.010	1.015	−0.5
25	0.947	0.962	−1.6
26	0.792	0.846	−6.8
27	0.720	0.766	−6.4
28	0.714	0.662	7.3
29	0.602	0.553	8.1
30	0.626	0.620	1.0

slightly enriched uranium fuels and contained 41 Vicor poison rods which were distributed in the core at regular intervals (Figure 9). In experiment the fuel rods were activated, and the gross fission product decay gammas of energy greater than 200 KeV were counted, using a collimated gamma-ray scintillation counter.

The result is summarized in Table 17. The calculated power distribution agrees excellently with the measured value along the north-south radius, but poorly at the midplane along the northwest radi us. The measured value is the

averge of two or more measurements along a given radius. Since the fuel rods were poorly positioned at the midplaane along the west and northwest radii[11], considerable dispersion can be seen in the measured data itself. Therefore, the discrepancy between the measured and calculated powers is belived to be originated from the measurement, not from the calculation.

IV. Conclusion and Recommendation

The adequacy of an analytical method utilizing KICC/KIDD code system has been verified

through extensive benchmark calculations against a series of critical experiments. The excellent agreements between the calculated and the measured power distributions as well as effective multiplication factors imply that the approximate treatments incorporated into KICC are correct and accurate.

Verification of CINDER depletion module incorprated into KICC is yet to be done and pre-requisite for the future work. The extension of KICC/KIDD system for the analysis of power reactor cores is also attempted as a future work.

References

1. Byung Jin Jun, Jonghwa Jang, Kap Suk Moon, Sang Keun Lee and Ji Bok Lee, "KICC: A Space-Dependent Cell Spectrum and Depletion Program for Analysis of Light Water Reactor Lattices, User's Manual," Korea Advanced Energy Research Institute (September 1983).

2. Sang Keun Lee, Ji Bok Lee, Chang Saeng Rim, Chang Kun Lee and Chang Hyun Chung, "An Effective Multiplication Factor Calculation of Uniform Lattices of UO_2-PuO_2 Fueled System," *Journal of the Korean Nuclear Society*, 14(3) pp. 138-147 (September 1982).

3. S.K. Lee et al., "KIDD, A KAERI Improved Diffusion-Depletion Program for Nuclear Reactor Analysis," Korea Advanced Energy Research Institute (to be published).

4. G.D. Joanou and J. S Dudek, "GAM-I: A Consistent P_1 Multigroup Code for the Calculation of Fast Neutron Spectra and Multigroup Constants," GA-1850 (June 1961).

5. H.C. Honeck, "THERMOS, A Thermalization Transport Theory Code for Reactor Lattice Calculations", BNL-5826 (September 1961).

6. T.R. England, "CINDER—A One-Point Depletion and Fission Product Program," WAPD-TM-334, Westrnghouse Electric Corporation(Revised June 1964).

7. J.R. Askew, "The Calculation of Resonance Capture in a Few Group Approximation," AEEW-R-489 (1966).

8. J.R. Askew, F.J. Fayers, and P.B. Kemshell, "A General Description of the Lattice Code WIMS," *Journal of the British Nuclear Society*, 5, 564 (1966).

9. H. Windsor and R. Goldstein, "Analysis of Lattices Containing Mixed Oxide Fuel in Particulate Form," *Trans. Am. Nucl. Soc.*, 15, 107 (1972).

10. J.R. Askew and R.J. Brissenden, "Some Improvements in the Discrete Ordinates Methods of B.G. Carlson for Solving the Neutron Transport Equation," AEEW-R-161 (1963).

11. R.H. Clark, M.L. Batch and T.G. Pitts, "Lumped Burnable Poison Program Final Report," BAW-3492-1, Babcoock and Wilcox (January 1966).

12. R.I. Smith and G.J. Konzek, "Clean Critical Experiment Benchmarks for Plutonium Recycle in LWR's, "EPRI-NP-196, Electric Power Research Institute (April 1976).

13. R.D. Leamer, et al, "PuO_2-UO_2 Fueled Critical Experiments, "WCAP-3726-1, Westinghouse Electric Corporation (July 1967).